ELSEVIER

### Contents lists available at ScienceDirect

# Desalination

journal homepage: www.elsevier.com/locate/desal





# Selective removal of heavy metals from saline water by nanofiltration

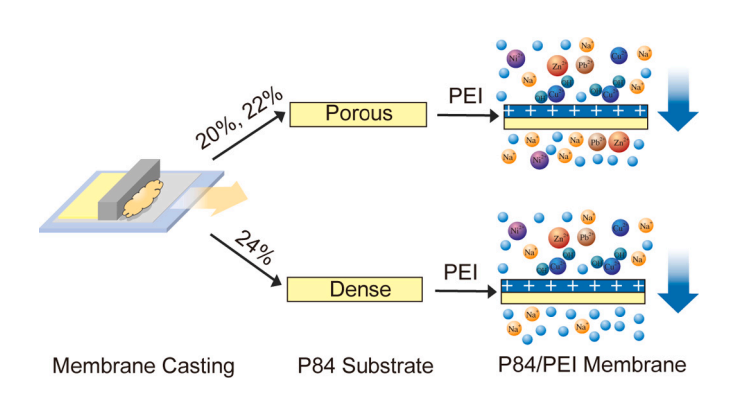
Junfeng Zheng <sup>a</sup>, Xin Zhang <sup>a</sup>, Guichuan Li <sup>b</sup>, Guanghai Fei <sup>c</sup>, Pengrui Jin <sup>a</sup>, Yanling Liu <sup>a,d</sup>, Christine Wouters <sup>a</sup>, Glen Meir <sup>a</sup>, Yi Li <sup>a,\*</sup>, Bart Van der Bruggen <sup>a,\*</sup>

- <sup>a</sup> Department of Chemical Engineering, KU Leuven, Celestijnenlaan 200F, 3001 Leuven, Belgium
- <sup>b</sup> Department of Materials Engineering, KU Leuven, 3001 Leuven, Belgium
- <sup>c</sup> Centre for Membrane Separations, Adsorption, Catalysis, and Spectroscopy for Sustainable Solutions (cMACS), KU Leuven, 3001 Leuven, Belgium
- <sup>d</sup> State Key Laboratory of Pollution Control and Resources Reuse, Tongji University, Shanghai 200092, China

### HIGHLIGHTS

- A positively charged nanofiltration membrane has been synthesized by cross-linking method.
- The pore size of membrane could be controlled by altering the concentration of P84 casting solutions.
- The 24%P84/PEI membrane showed a high selective removal of heavy metals from saline water.

### GRAPHICAL ABSTRACT



### ARTICLE INFO

Keywords: P84 membrane Polyethylenimine (PEI) Heavy metals Ion-ion selective Saline water

### ABSTRACT

Polyethylenimine (PEI) cross-linked P84 nanofiltration membranes were successfully developed through a facile stirring cross-linking method. The separation performance of the membrane was tailored by changing the concentration of the P84 casting solution. A systematic characterization, including chemical structure, surface morphology, surface charge, and separation performance, was carried out. Nanofiltration membranes with a high positive charge and hydrophilic surface were successfully fabricated. All the PEI cross-linked membranes showed high isoelectric points at pH from 8 to 8.9 and a mean pore radius from 0.389 to 0.474 nm. Under the influence of the Donnan effect and size exclusion, the 20%P84/PEI membrane showed an excellent water permeance of 27.7  $\pm$  1.5 L m $^{-2}$  h $^{-1}$  bar $^{-1}$  and a high rejection (>90%) for single-component heavy metal salts (ZnCl<sub>2</sub>, PbCl<sub>2</sub>, Ni (NO<sub>3</sub>)<sub>2</sub> and Cu(NO<sub>3</sub>)<sub>2</sub>). A variety of mixed salt separation performance tests were performed. These results clearly indicate that the 20%P84/PEI and 22%P84/PEI membranes have a huge potential to remove and concentrate copper ions from aqueous solutions. In particular, the 24%P84/PEI membrane is promising in the selective removal of various heavy metals from highly saline water.

E-mail addresses: yili.kuleuven@gmail.com (Y. Li), bart.vanderbruggen@kuleuven.be (B. Van der Bruggen).

<sup>\*</sup> Corresponding authors.

#### 1. Introduction

Heavy metals, such as copper, lead, cadmium, and zinc are toxic, non-biodegradable, and accumulate easily in living organisms, threatening public health and the environment [1–3]. Even for plant systems, contaminations of heavy metals could alter the activity of several enzymes, causing growth retardation and disturbing photosynthesis [4]. With industrialization, wastewater discharge is one of the primary sources of heavy metal discharged into the environment [5]. Therefore, removing heavy metals from wastewater attracts tremendous social attention.

Membrane separation, coagulation-flocculation, precipitation, ionic exchange, and adsorption are the conventional technologies for removing heavy metals from wastewater [6]. Each of these techniques has its advantages and scope of applications. However, some unavoidable limitations prompt researchers to seek advanced technologies and improve these existing technologies to achieve a more efficient separation of heavy metals from wastewater [6]. Compared with conventional techniques, membrane separation technology offers several advantages: low energy consumption, no addition of chemicals, environmentally friendly, and mature large-scale application [7].

Nanofiltration membrane, one of the pressure-driven membrane separation technologies positioned between ultrafiltration and reverse osmosis, has a small pore size of 0.5-2 nm with a molecular weight cutoff (MWCO) between 200 and 1000 Da [8]. It has a lower operating pressure than reverse osmosis due to the loose selective layer and a better ion selectivity than ultrafiltration due to the appropriate pore sizes [9]. The separation mechanism is mainly considered to be the size exclusion and the Donnan effect [10,11]. These features have made nanofiltration a promising process for separating metallic ions from wastewater [12-14]. Today, the mainstream nanofiltration membranes are made of aliphatic amine monomers with trimesoyl chloride (TMC) prepared by interfacial polymerization (IP) upon a support substrate. In general, these membranes show a negatively charged surface due to the hydrolysis of the unreacted acyl chloride groups of TMC. Due to the Donnan effect, the negatively charged membranes have a higher rejection towards multivalent anions and a lower rejection of multivalent cations, which is not conducive to removing heavy metals [15]. Therefore, developing a positively charged nanofiltration membrane is a good strategy for removing heavy metal ions.

Poly(ethylenimine) (PEI), a water-soluble polyelectrolyte containing abundant primary and secondary amine groups, is a good candidate for preparing positively charged nanofiltration membranes. For instance, Chiang et al. prepared a positively charged nanofiltration membrane by an IP reaction between hyperbranched PEI and TMC [16]. More recently, Zhang et al. incorporated hydroxyl contained multi-walled carbon nanotubes in the PEI solution via an IP with TMC to synthesis a positively charged nanofiltration membrane. The optimal membrane has a high rejection around 97% for divalent cations and low rejection less than 70% for monovalent cations [17]. Even though the abundant  $^{\rm -NH_3^+}$  and  $^{\rm -NH_2^+}$  make the membrane surface positively charged, the hydrolysis of some residual acyl chloride groups still reduces the positive charge on the membrane surface.

Compared with conditional IP procedures, the cross-linking reaction between PEI and the polyimide substrate can easily proceed through the ring-opening reaction on the backbone of polyimide [18]. P84 (copolyimide of 3,3',4,4'-benzophenone tetracarboxylic dianhydride with 80% toluene diisocyanate and 20% methylphenylenediisocyanate) was used as the polyimide substrate because it is thermally stable, chemically durable, and chemically resistant in organic solvents or acidic/basic conditions. The hyperbranched PEI can introduce plenty of -NH2 and -NH- groups on the surface and the inner pores of the membrane, making the membranes highly positively charged. Consequently, the introduced PEI not only excludes cations through the Donnan effect but also reduces the pore size of the membranes.

There is an increasing demand for separating heavy metals from

brine water, such as electroplating wastewater, removing heavy metal ions from industrial wastewater and saline-alkali water, and recycling metals from city mines [15,19]. In these cases, multivalent cations need to be separated from a mixed salts solution. Most of the current research is aimed at the separation of single-component salts [20–22]. To date, a very few research on the separation of heavy metals from high-concentration saline solution using positively charged nanofiltration membranes was reported. Therefore, it is essential to synthesize a highly positively charged membrane with a controllable pore size through a simple fabrication process to realize selective separation.

In this work, we prepared a positively charged nanofiltration membrane by a chemical cross-linking reaction on top of a P84 substrate. The pore size of the cross-linked membrane was controlled by altering the concentration of P84 casting solutions. The separation performances of the as-prepared membrane for single-component and mixed-component salts with different concentrations have been systematically evaluated. Depend on the Donnan effect and size exclusion, the PEI cross-linked membrane realized the efficient separation of heavy metals from saline water. Characteristics, such as chemical composition, morphology, contact angles, pore size distribution, and zeta potentials, were also investigated and discussed.

### 2. Experimental

# 2.1. Materials

Polypropylene/polyethylene nonwoven fabrics (Novatexx 2471) with a thickness of 0.18 mm were acquired from Freudenberg Group (Germany). P84 polymer powders (MW:153000 g mol $^{-1}$ ) were purchased from HP Polymer GmbH, Austria. Branched PEI (average Mw  $\sim$ 25,000 by LS, average Mn  $\sim$  10000 by GPC) was obtained from Sigma-Aldrich (Diegem, Belgium). N, N-dimethylformamide (DMF) 1,4-dionane was purchased from BAKER ANALYZED Reagent. N-dimethylformamide (DMF, 99.8%), sodium chloride (NaCl, 99%), sodium sulfate (Na<sub>2</sub>SO<sub>4</sub>, 99%), magnesium chloride (MgCl<sub>2</sub>), magnesium sulfate (MgSO<sub>4</sub>, 99%), zinc chloride (ZnCl<sub>2</sub>, 98+%), lead chloride (PbCl<sub>2</sub>, 98%), glucose (99.5%), maltose monohydrate (99%) and raffinose pentahydrate (99%) were purchased from Sigma-Aldrich. Nickel nitrate hexahydrate (Ni(NO<sub>3</sub>)<sub>2</sub>, 99%) and copper nitrate trihydrate (Cu(NO<sub>3</sub>)<sub>2</sub>, 99%) were obtained from Acros Organics. Deionized water was used throughout this study.

### 2.2. Synthesis of asymmetric porous substrate

The P84 substrate was prepared via a traditional phase inversion method. In detail, P84 polymer casting solutions with a concentration of 20 wt%, 22 wt%, and 24 wt% were prepared by dissolving P84 powder in a mixture of 1,4-dionane and DMF (1:4 in weight). The casting solution was then cast onto a nonwoven fabric using a doctor blade with a gap thickness of 250  $\mu m$ . After a 60 s air bath ( $\sim\!25\,^{\circ}\text{C}$ , relative humidity of 33%  $\pm$ 5%), the membrane was immersed into the water bath for at least 30 min. Finally, the membranes were washed thoroughly and then stored in deionized water before further modifications. Membranes prepared in this step were named 20%P84, 22%P84, and 24%P84 substrate, respectively, according to the P84 polymer concentration.

### 2.3. Preparation of the PEI cross-linked nanofiltration membranes

The prepared P84 substrates were cut into pieces of 5 cm in diameter. Then, the cut membrane was immersed into a 100 mL container bottle with 50 mL PEI aqueous solution (15 g  $\rm L^{-1})$  equipped with a magnetic rotor stirring at 100 rpm; the curled side of the membrane was facing up. After cross-linking with branched PEI for 20 h at  $\sim\!25~^{\circ}\text{C}$ , the resultant membranes were rinsed and stored in deionized water before testing. Membranes were named 20%P84/PEI, 22%P84/PEI, and 24%P84/PEI membrane, respectively, according to the P84 substrate.

#### 2.4. Characterization

All membrane samples were dried in a vacuum oven at 40 °C overnight. It should be noted that the membrane samples need to be fixed when drying because they are easy to bend. The chemical composition of membranes was measured by ATR-FTIR (PerkinElmer Spectrum 100, Germany) and X-ray photoelectron spectroscopy (XPS, AMICUS/ESCA 3400 system). Surface and cross-section micrographs of membranes were obtained using an FEI Nova NanoSEM 450 scanning electron microscope (SEM) at an acceleration voltage of 10 kV. The surface roughness of all membranes was measured by atomic force microscopy (AFM, Dimension Icon SPM, Veeco Instruments Inc.). The surface charge of all prepared membranes was measured by a zeta potential machine (SurPASS 2.0, Anton Paar, Australia). The concentrations of heavy metal ions were evaluated by Inductive Coupled Plasma-Mass Spectrometry (Perkin Elmer ICP-MS, Nexion 5000). The dynamic water contact angle of membrane surface was measured by a DataPhysics Instruments OCA 20 Optical Contact Angle Meter (Germany). The solid-liquid interfacial free energy  $(-\Delta G_{SL})$  indicating the wettability of the membrane surface was calculated according to the Young-Dupre equation [23], as shown in

$$-\Delta G_{SL} = \gamma_L \left( 1 + \frac{\cos \theta}{s} \right) \tag{1}$$

where  $\gamma_L$  represents the surface tension of water at 25 °C (72.8 mJ m<sup>-2</sup>);  $\theta$  is the water contact angle; s is the roughness factor, which is defined as the ratio the real surface area to the projected area (scanning area in the AFM measurement).

### 2.5. Filtration performance measurement

A lab-scale METcell cross-flow system (an active membrane area of  $14.6~{\rm cm}^2$ , Evonik, UK) was applied to evaluate the membrane separation performances at room temperature (~25 °C). The set-up has a cross-flow rate of  $1.2~{\rm L~min}^{-1}$  (solution with a viscosity of  $1.0~{\rm cP}$ ) and consists of a stainless-steel feed tank, a high-pressure diaphragm pump (LAFERT type AMM 71Z, and Micropump L22479 GC-M23.JF5S.6 Gear Pump Pumphead), two pressure gauges, two bypass valves, and other accessories. Lab-scale dead-end equipment (an active membrane area of  $14.6~{\rm cm}^2$ , HP4750) was employed as the contrast. An electric magnetic stirrer was used in a stirring speed of 500 rpm to minimize the concentration polarization at room temperature during the tests.

Two test pressures, 4 bar and 8 bar, were used throughout this study. 4 bar was used for single-component salts  $(MgCl_2, NaCl, Na_2SO_4, and MgSO_4 of 1000 mg L^{-1}; ZnCl_2, PbCl_2, Ni(NO_3)_2 and Cu(NO_3)_2 of 250 mg L^{-1}), pre-pressurized at 8 bar for at least 0.5 h to stabilize the water flux. 8 bar was used for all mixed salts and high concentration of Na<sub>2</sub>SO<sub>4</sub> (5, 10, and 20 g L<sup>-1</sup>), pre-pressurized at 12 bar for at least 0.5 h.$ 

The water permeance (*WP*, L m<sup>-2</sup> h<sup>-1</sup> bar<sup>-1</sup>) and solute retention values (*R*, %) of the membranes were calculated as follows:

$$WP = \frac{V}{A\Delta t \Delta P} \tag{2}$$

$$R(\%) = \left(1 - \frac{Cp}{Cf}\right) \times 100\tag{3}$$

where V (L) is the volume of the collected permeate in a time interval of  $\Delta t$  (h); A (m<sup>2</sup>) is the effective membrane area, and  $\Delta P$  (bar) represents the transmembrane pressure. Cp (mg L<sup>-1</sup>) and Cf (mg L<sup>-1</sup>) refer to the concentration of the permeance solution and the feed solution, respectively. Concentrations of single-species, such as Na<sub>2</sub>SO<sub>4</sub>, MgSO<sub>4</sub>, MgSO<sub>4</sub> and NaCl, were measured by Electrical Conductivity equipment (UT30B, Shenzhen Uni-trend Electronics Company). For the mixed-salt solutions, Inductive Coupled Plasma-Mass Spectrometry (Perkin Elmer ICP-MS, Nexion 5000) was used to analyze the concentrations of different salt

ions.

# 2.6. Pore size distribution

The pore size distribution of the prepared membranes was measured by the separation of neutral organic solutes, i.e., glucose (180.2 Da), sucrose (342.3 Da), and raffinose (504.4 Da), 5000 ppm. The sugar concentrations were measured using High-Performance Liquid Chromatography (HPLC, Shimadzu Prominence-i LC-2030C 3D). The sugar rejection was calculated by using the mentioned equation above (3).

By assuming there are no hydrodynamic and electrostatic interactions between the solute and membrane pores during the filtration process, the mean effective pore radius ( $\mu p$ ) of the membrane can be considered the Stokes radius of a solute when the rejection of the solute is 50%. The geometric standard deviation ( $\sigma p$ ) of the membrane is defined as the ratio of the solute radius when R = 84.1% over R = 50%. The relation between the pore size distribution of the membrane and solute Stokes radius was mathematically fitted by the following Eq. (4) [24,25].

$$\frac{df(r_p)}{dr_p} = \frac{1}{r_p ln \sigma_p \sqrt{2\pi}} exp \left[ -\frac{(ln r_p - ln \mu_p)^2}{2(ln \sigma_p)^2} \right]$$
(4)

where  $r_p$  is the pore size of the membrane.

### 3. Results & discussion

#### 3.1. Fabrication of PEI cross-linked membranes

Fig. 1 displays the chemical structure of P84 copolyimide, branched PEI, and the possible structure of the cross-linked membranes. According to previous research, a defect-free positively charged membrane can be prepared by immersing the P84 substrate in a PEI aqueous solution at room temperature for up to 20 hours with gentle stirring [45]. An optimal cross-linker concentration, cross-linking time, and temperature were achieved regarding the excellent removal efficiency of copper ions in water. However, the separation of heavy metal ions from salt ions, especially in highly saline water, remains challenging and requires systematic research work. Furthermore, it was found that the P84 concentration greatly affects the membrane's separation performance. To explore the appropriate polymer concentration for better separation of heavy metals, three casting solutions containing 20 wt%, 22 wt%, and 24 wt% polymers were used to prepare P84 substrates by the phase inversion method. Afterwards, the resultant three P84 substrates were immersed in a 15 g L<sup>-1</sup> PEI aqueous solution, respectively, for chemical modification, as described in the method part.

The chemical cross-linking reaction between the P84 substrates and P84/PEI membranes was confirmed by FTIR and XPS analyses. Fig. 2(a) shows the FTIR spectroscopy (2000–1200 cm<sup>-1</sup>) of P84 substrates and P84/PEI membranes. Before the PEI cross-linking, all of the three P84 substrates have similar absorption peaks at 1780 cm<sup>-1</sup> (C=O stretching), 1718 cm<sup>-1</sup> (C=O stretching), and 1360 cm<sup>-1</sup> (C=N stretching) attributed to the presence of imide groups [26]. After PEI cross-linked, the absorption peaks of the imide diminished but not disappeared, which suggests that there are unreacted imide groups. The three PEI cross-linked membranes exhibit two new peaks at around 1648 cm<sup>-1</sup> and 1535 cm<sup>-1</sup>, corresponding to the C=O stretching and C=N stretching of amide groups [27]. The higher wavenumber regimes of FTIR spectroscopy (4000–1000 cm<sup>-1</sup>) are shown in Fig. S1. The broad peak at around 3000–3500 cm<sup>-1</sup> (N=H vibrations) for P84/PEI membranes could be attributed to the presence of free amine groups [26].

The XPS spectrum gives further evidence of the successful modification of PEI on the P84 membranes. As shown in Fig. 2(b), the increase in N1s content for 20%, 22%, and 24% P84/PEI membranes suggests that the PEI had successfully cross-linked the top active layer of the membrane. The C1s, N1s, and O1s proportion of pristine and cross-

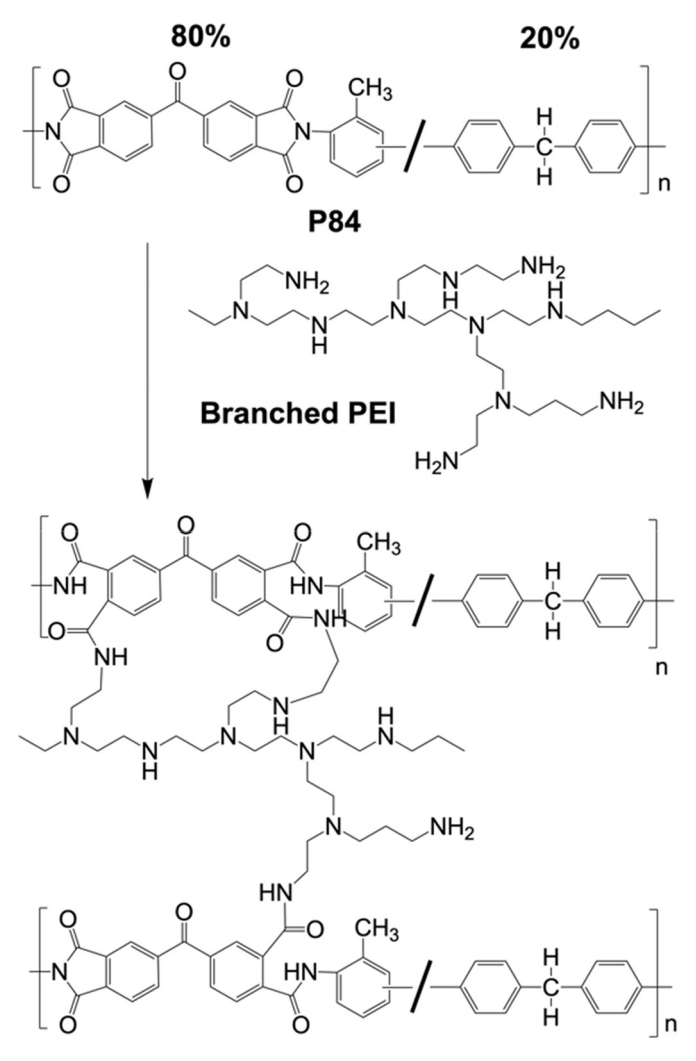


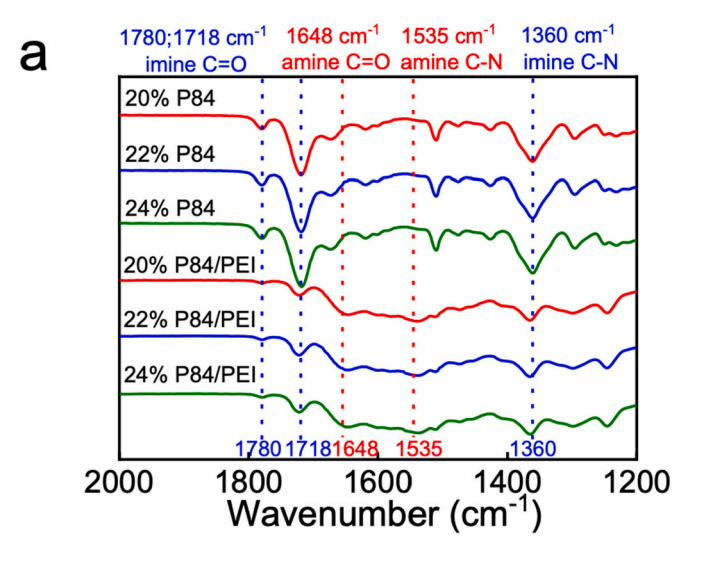
Fig. 1. The chemical reaction between P84 and branched PEI.

linked membranes were obtained from XPS spectrum, as shown in Table 1. The N1s to O1s ratio (N/O) could reveal the degree of PEI cross-linking [27]. After PEI modification, the N/O ratio elevated from 0.39, 0.43 and 0.25 to 1.10, 0.87 and 0.83 for 20%, 22% and 24% P84 membranes, respectively. This indicates that the PEI is well cross-linked with the P84 substrate and has a similar cross-linking degree for the three membranes prepared in different polymer concentrations.

### 3.2. Characterization of PEI cross-linked membranes

The transport mechanism for nanofiltration membranes is generally dominated by the size exclusion and the Donnan effect [11]. There exist strong hindrances of ion transporting through the pores of the membrane when the ionic radius of a given ion in the feed is larger than the pore radius of the membrane [24]. In contrast, an ion with a small size would pass through the membrane, leading to a low rejection. Thus, a high ion-ion selectivity could be expected if the pore size of the membrane is finely controlled. Inspired by this, the membrane pore size was tailored by changing the concentration of P84. Apart from this, heavy metal ions are generally multivalent cations, such as Cu<sup>2+</sup>, Ni<sup>2+</sup>, Pb<sup>2+</sup>, and Cr<sup>3+</sup>. Considering the Donnan effect, a positively charged membrane has a high retention for the multivalent cations. Based on these views, a series of positive membranes were fabricated by the crosslinking reaction of PEI and P84 substrate in view of separating metallic ions from saline water.

The separation performance of the positively charged membranes



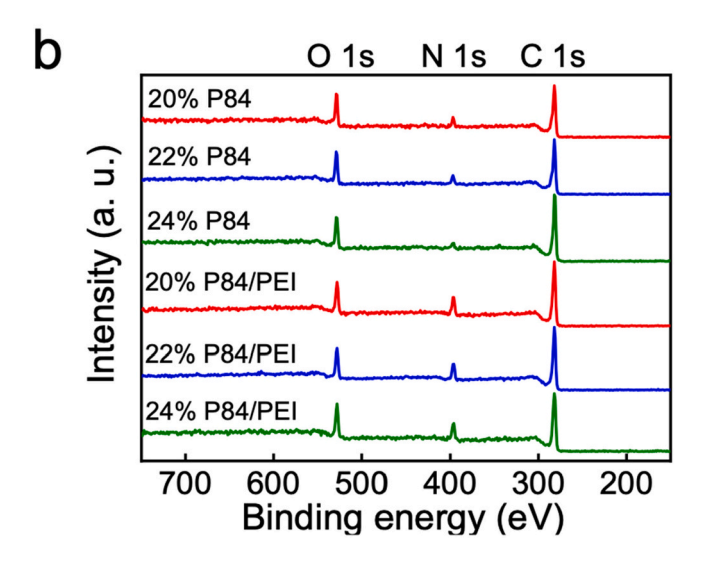


**Fig. 2.** Chemical composition of the membranes. (a) ATR-FTIR spectra and (b) XPS results.

Table 1
XPS results of P84 substrates and PEI cross-linked membranes.

Item	C (%)	O (%)	N (%)	N/O
item	C (%)	0 (%)	IN (%)	N/O
20%P84	81.63	5.15	13.22	0.39
22%P84	82.93	5.13	11.94	0.43
24%P84	84.77	3.08	12.15	0.25
20%P84/PEI	78.68	11.16	10.15	1.10
22%P84/PEI	81.40	8.63	9.97	0.87
23%P84/PEI	77.67	10.10	12.23	0.83

was measured in a lab-scale crossflow setup with a typical MgCl $_2$  solution (1000 mg L $^{-1}$ ). Fig. 3 displays the pure water flux, salt solution flux, and MgCl $_2$  rejection of the PEI cross-linked membranes with different P84 concentrations of 20%, 22%, and 24%. It was found that when the P84 concentration was 20%, the cross-linked membrane had the highest pure water permeance of 27.7  $\pm$  1.5 L m $^{-2}$  h $^{-1}$  bar $^{-1}$  and a lower MgCl $_2$  rejection of  $\sim$ 90%. In contrast, the 24%P84/PEI membrane exhibited a low pure water permeance of 9.1  $\pm$  0.6 L m $^{-2}$  h $^{-1}$  bar $^{-1}$  but a high MgCl $_2$  rejection of 95.7  $\pm$  0.8. The permeability and selectivity of the 22%P84/PEI membrane is between that of the above two membranes (i. e., MgCl $_2$  rejection of 93.9  $\pm$  1.3 and water permeance of 23.0  $\pm$  1.2 L m $^{-2}$  h $^{-1}$  bar $^{-1}$ ). In comparison, the 22%P84/PEI membrane was

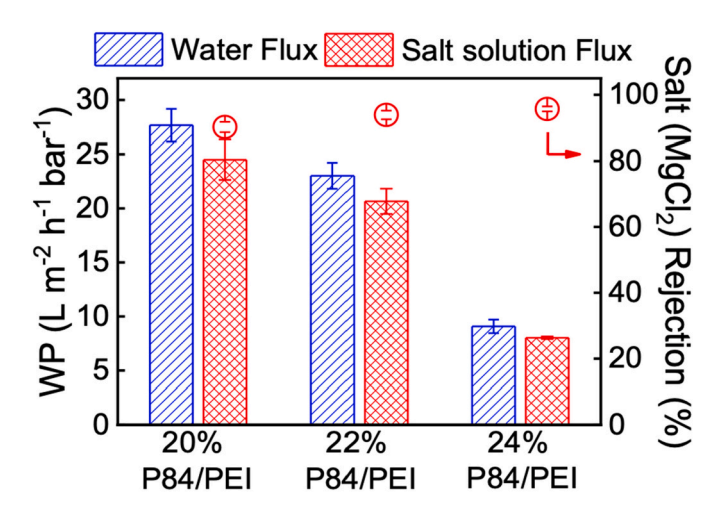


Fig. 3. Separation performance of PEI cross-linked P84 membranes (1000 mg  $L^{-1}$  of MgCl<sub>2</sub> solution, 25 °C, 4 bar).

evaluated by the dead-end setup in the same test condition (Fig. S2). Due to the high cross-flow rate  $(1.2~L~min^{-1})$  of the METcell cross-flow system, the cross-flow filtration mode has significant advantages in both flux and rejection for a given membrane compared with the dead-end filtration mode.

The three PEI cross-linked membranes have the same level of MgCl<sub>2</sub> rejections but a different water permeance, corresponding to different membrane hydraulic resistances. To explore this phenomenon, the membrane morphology was characterized, assuming that it significantly impacts the water permeance of the membranes. Fig.  $4(a_1-f_1)$  presents the cross-sectional SEM images of the P84 substrates and the P84/PEI nanofiltration membranes with different concentrations of P84 casting solutions. The FESEM image of a larger magnification is displayed in Fig. S3, to give more fundamental information about the morphology of the membrane. There is no apparent difference among the three P84 substrates. However, the cross-section of the membranes has a dividing line after the PEI cross-linking, which indicates that the PEI has successfully penetrated into the membrane pores and cross-linked the top layer of the P84 membrane. Therefore, it should be assumed that this thick top layer is an active barrier layer of the P84/PEI nanofiltration membrane. In addition, the thickness of the three cross-linked layers is similar, around 1 um. This finding indicates that the thickness of the cross-linked active layer is not closely related to the concentration of the P84 casting solution. Notably, membrane hydraulic resistances are directly governed by their thickness [28]. Combining the N/O ratios of the three PEI cross-linked membranes, it can be concluded that the crosslinking degree and the thickness of the PEI cross-linked layer are not the dominant factors determining the differential water permeability.

Fig. 4(a<sub>2</sub>–f<sub>2</sub>) displays the surface SEM images of all the membrane samples. The plain P84 substrates have a smooth surface. After the reaction with the PEI, the morphology of the membrane surfaces shows a protuberant structure. This is also reflected by the AFM results, as shown in Fig. 4(a<sub>3</sub>–f<sub>3</sub>). The 20%P84, 22%P84, and 24%P84 substrates show an almost smooth surface, with a root-mean-square roughness of 3.48  $\pm$  0.01 nm, 3.41  $\pm$  0.05 nm, and 2.84  $\pm$  0.18 nm, respectively (Table S1). In comparison, the PEI-covered membrane has a relatively rough surface, demonstrating that the PEI molecules anchored and agglomerated on the surface of the membrane [29]. However, the root-mean-square roughness of the three PEI cross-linked membranes was similar in this study (Table S1).

The hydrophilicity of a membrane surface has a vital influence on its water permeance. To better understand the relationship between surface hydrophilicity and water permeance of the membranes, the dynamic and static water contact angles (WCAs) were measured (see Fig. 5). A lower water contact angle indicates a hydrophilic membrane surface and

vice versa [30]. Focusing on the 20%P84, 20%P84, and 20%P84 substrate, it could be found that the 24%P84 substrate displays the most hydrophobic surface in terms of the dynamic and static water contact angle, while the 20%P84 substrate is the most hydrophilic. This is because a dense structure of the membrane tends to be hydrophobic compared with a porous structure [31]. After PEI cross-linking, the WCA of all the P84 (20%, 22%, and 24%) substrate decreased, indicating that the hydrophilic PEI was successfully grafted on the P84 substrate. The hydrophilicity of PEI cross-linked membranes follows the order of 20% P84/PEI > 22%P84/PEI > 24%P84/PEI, which is consistent with the water permeance of the above membranes. The roughness of the membrane influences the water contact angle of the membrane. The interfacial free energy covers the effects of the surface morphology and the surface energy, giving a more fundamental insight into the membrane wettability than the raw WCA results [23]. Compared with the P84 substrate as shown in Fig. 5(b), the PEI cross-linked membranes have an increased -  $\Delta G_{SL}$ , suggesting a higher affinity to water molecules. The order of the surface free energy of the three PEI cross-linked membranes also coincides with their water permeance results. Specifically, the pore size of the membrane is another important factor that governs the membrane flux except in the case of a loose membrane.

#### 3.3. Separation performance of PEI cross-linked membranes

The separation performance of the three PEI/P84 membranes was systematically tested using four typical inorganic salts (NaCl, MgCl<sub>2</sub>, Na<sub>2</sub>SO<sub>4</sub>, and MgSO<sub>4</sub>). The results are shown in Fig. 6(a). It could be found that the three membranes have the same rejection sequence, MgCl<sub>2</sub> > MgSO<sub>4</sub> > NaCl > Na<sub>2</sub>SO<sub>4</sub>, representing a typical positively charged surface. The electrokinetic analyzer was used to measure the streaming potential of the membrane surface in a pH range of 2-10 as shown in Fig. 7. The isoelectric points (IEP) of the 20%P84, 22%P84, 24%P84, 20%P84/PEI, 22%P84/PEI, and 24%P84/PEI membranes are at the pH of 3.0, 3.1, 2.8, 8.5, 8.0, and 8.9, respectively. The positive charge of the cross-linked P84 membranes is because of the protonation of the unreacted amine groups from the branched PEI and the newly formed amide groups between P84 and PEI [27]. To maintain the charge balance in the solution, the repulsion of magnesium salt (MgCl2 and MgSO<sub>4</sub>) by the positively charged NF membrane is larger than that of sodium salt (NaCl and Na<sub>2</sub>SO<sub>4</sub>). In addition, sodium ions, with a smaller hydration radius (0.358 nm) compared with magnesium ions (0.428 nm), preferentially permeate through the membrane. The positively charged membrane has a higher rejection for chlorides (MgCl2 and NaCl) than for sulfates (MgSO<sub>4</sub> and Na<sub>2</sub>SO<sub>4</sub>). The is because the repulsive interactions between cation ions the membrane surface are partially shielded by the adsorbed dual charged (SO<sub>4</sub><sup>2-</sup>) ions, resulting in a much weakened electrostatic repulsion [32,33]. Specifically, among the three PEI cross-linked membranes, the 20%P84/PEI membrane has the highest water permeance, while the 24%P84/PEI membrane has the best rejection to all four types of salts.

The pore size of a membrane determines the size exclusion effect.. The pore size distribution of membranes was calculated according to the Stokes radius of glucose, sucrose, and raffinose; this is shown in Fig. 8 [35]. As expected, the mean pore radius of the PEI cross-linked membrane has a declining trend with the increased concentration of the P84 polymer. The mean pore radius of 20%P84/PEI, 22%P84/PEI, and 24% P84/PEI was calculated to be 0.474 nm, 0.426 nm, and 0.389 nm, respectively. The mean pore radius of the 20%P84/PEI membrane is larger than the hydrated radii of Mg<sup>2+</sup> (0.428 nm). However, the membrane still maintains a good rejection of MgCl2 of over 90%, suggesting that the Donnan effect dominates the separation. Note that the rejection of a single salt is entirely different from the rejection of mixed salts. The separation performance of the membrane with mixed salts is discussed in the next section. The 24%P84/PEI membrane has the highest salt rejection and the lowest water permeance due to the dense structure. It was concluded that the concentration of the casting solution

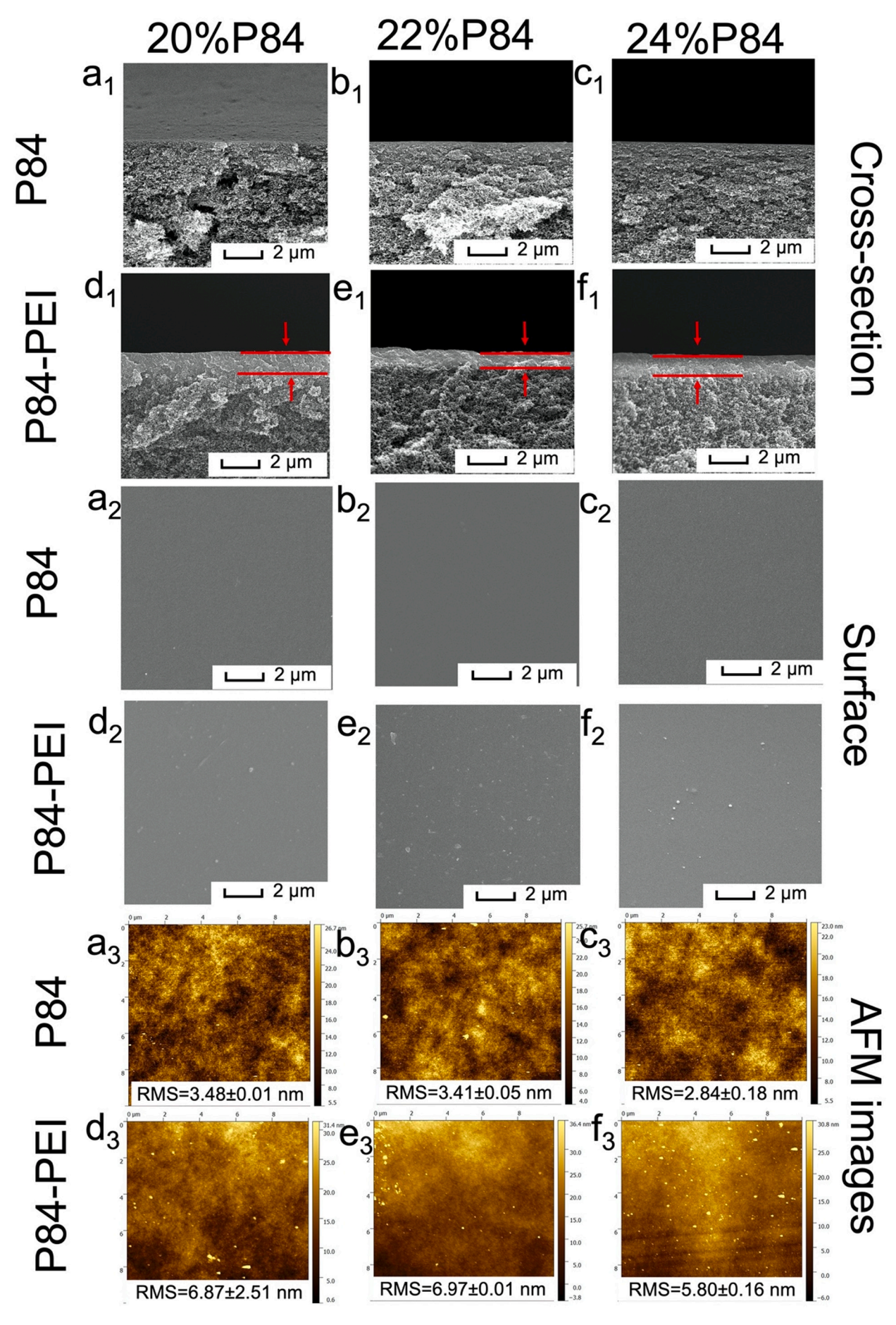
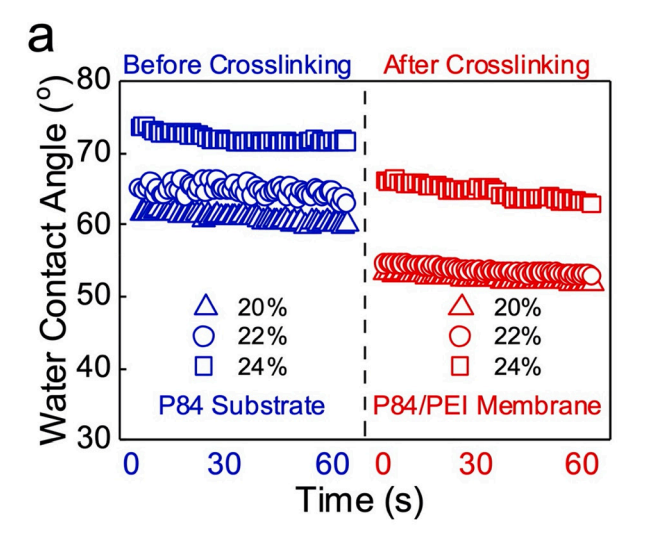
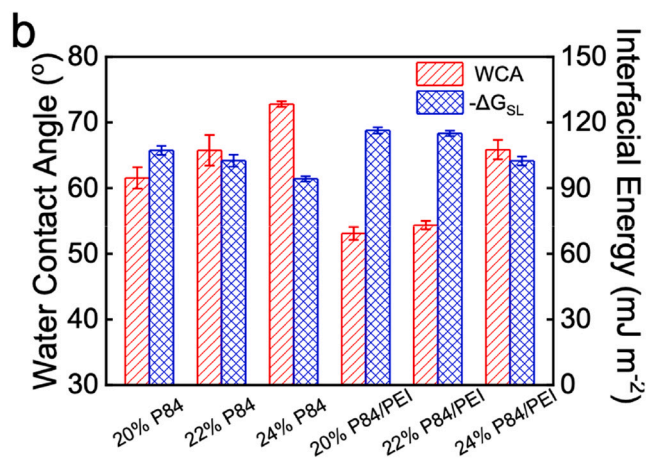


Fig. 4. Morphology of P84 substrates and PEI cross-linked membranes. Cross-sectional FESEM images of (a<sub>1</sub>) 20%P84, (b<sub>1</sub>) 22%P84 and (c<sub>1</sub>) 24%P84 substrate; (d<sub>1</sub>) 20%P84/PEI, (e<sub>1</sub>) 22%P84/PEI, and (f<sub>1</sub>) 24%P84/PEI membrane. Top surface FESEM images of (a<sub>2</sub>) 20%P84, (b<sub>2</sub>) 22%P84, and (c<sub>2</sub>) 24%P84 substrate; (d<sub>2</sub>) 20%P84/PEI, (e<sub>2</sub>) 22%P84/PEI, and (f<sub>2</sub>) 24%P84/PEI membrane. AFM observations of (a<sub>3</sub>) 20%P84, (b<sub>3</sub>) 22%P84, and (c<sub>3</sub>) 24%P84 substrate; (d<sub>3</sub>) 20%P84/PEI, (e<sub>3</sub>) 22%P84/PEI, and (f<sub>3</sub>) 24%P84/PEI membrane.



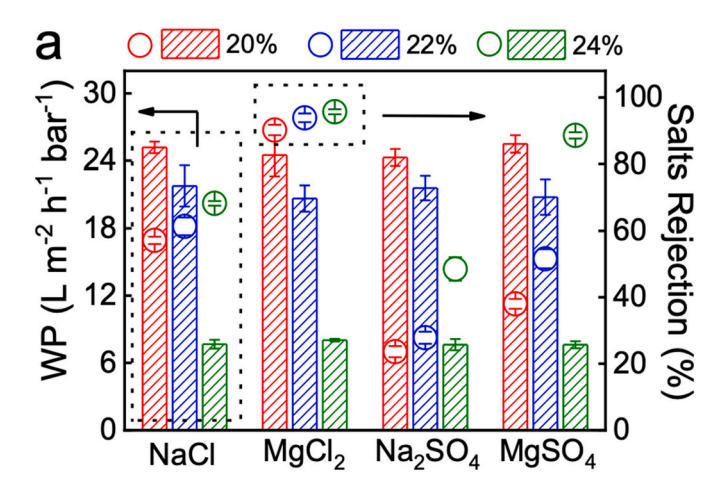


**Fig. 5.** (a) Dynamic WCAs of the membrane surface. (b) Static WCAs and interfacial free energy of membranes (the static WCAs was the data when the droplet touched the membrane surface at 10 s).

could effectively tune the pore size of the membrane without sacrificing the surface charge (Fig. 7).

Considering the high rejection of the positively charged membranes for divalent cations, four common heavy metal ions,  $\text{Cu}^{2+}, \, \text{Ni}^{2+}, \, \text{Zn}^{2+},$  and  $\text{Pb}^{2+},$  were used to manifest the removal efficiency of the developed P84/PEI membrane for heavy metal cations. The three PEI cross-linked membranes show a high rejection for all heavy metal salts, ZnCl<sub>2</sub>, PbCl<sub>2</sub>, Ni(NO<sub>3</sub>)<sub>2</sub>, and Cu(NO<sub>3</sub>)<sub>2</sub>, as presented in Fig. 6(b). Especially, the rejection of the 24%P84/PEI membrane to all heavy metal salts is above 98.5%. The hydrated radius of the ions of concern is displayed in Table 2, showing the order  $\text{Zn}^{2+} > \text{Cu}^{2+} > \text{Ni}^{2+} > \text{Pb}^{2+}$ . However, Fig. 6 (b) displays a totally different rejection order, Cu(NO<sub>3</sub>)<sub>2</sub> > PbCl<sub>2</sub> > ZnCl<sub>2</sub> > Ni(NO<sub>3</sub>)<sub>2</sub>. Therefore, other factors should be considered.

Based on the solution-diffusion model, the solute firstly sorbs on the membrane surface on the feed side and diffuses through the membrane matrix. Finally, the solute desorbs at the permeate side of the membrane. Thus, the separation efficiency is governed by the solubility and diffusivity of the solutes. As reported by Zhang et al., a negatively charged membrane could result in electrostatic attraction and enhance transport



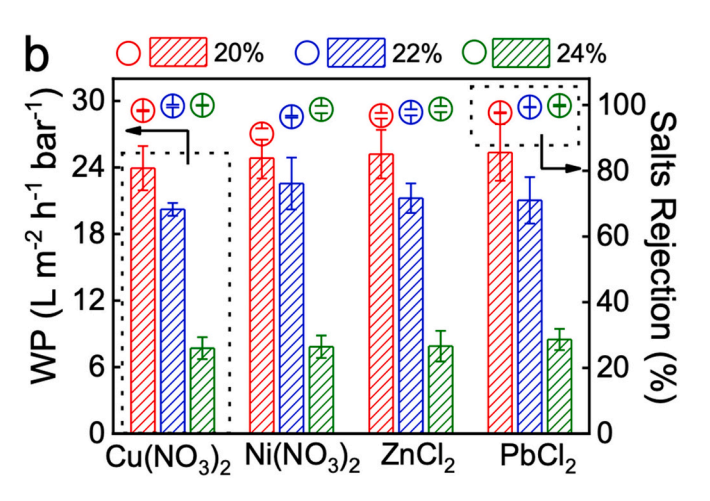


Fig. 6. Separation performance of PEI cross-linked membranes. (NaCl, MgCl<sub>2</sub>, Na<sub>2</sub>SO<sub>4</sub> and MgSO<sub>4</sub> of 1000 mg L<sup>-1</sup>; ZnCl<sub>2</sub>, PbCl<sub>2</sub>, Ni(NO<sub>3</sub>)<sub>2</sub> and Cu(NO<sub>3</sub>)<sub>2</sub> of 250 mg L<sup>-1</sup>, 25 °C, 4 bar.)

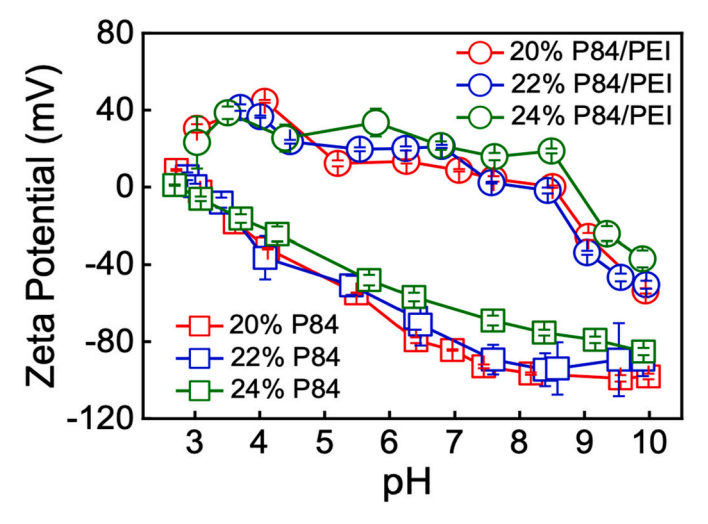


Fig. 7. Zeta potentials of the P84 substrate and P84/PEI membranes.

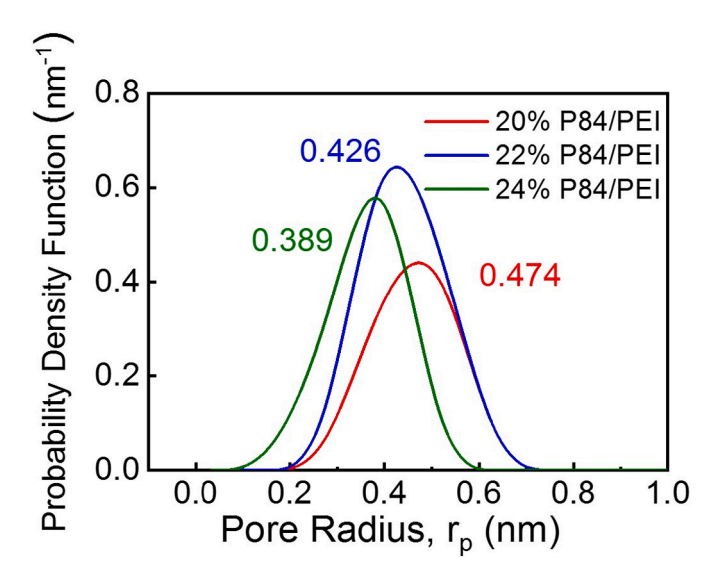


Fig. 8. Probability density function curves of different P84/PEI membranes. (The filtration data were collected from 0.5 h at 25  $^{\circ}$ C, 4 bar.)

Table 2 Physical properties (hydrated radius, diffusion coefficient) of various ions used in this work (at  $25 \,^{\circ}$ C [34]).

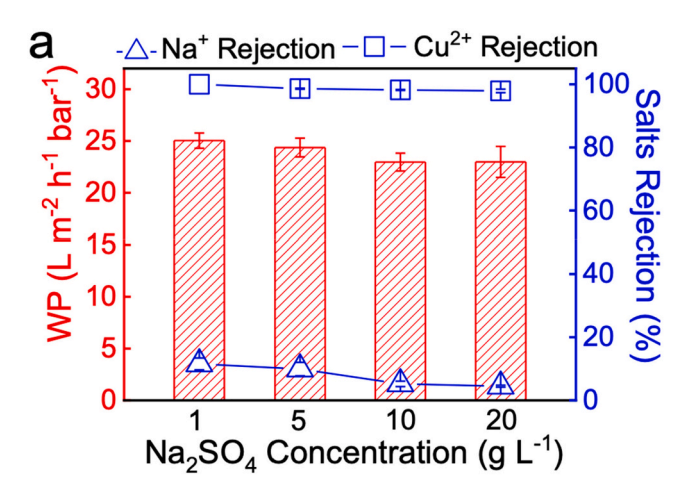
Type of ions	Hydrated radius (nm)	Diffusivity ( $10^{-9} \text{ m}^2 \text{ s}^{-1}$ )
Na <sup>+</sup>	0.358	1.33
${ m Mg}^{2+}$ ${ m Pb}^{2+}$	0.428	0.72
	0.401	0.95
Ni <sup>2+</sup>	0.404	0.68
$Zn^{2+}$	0.430	0.71
Cu <sup>2+</sup>	0.419	0.72

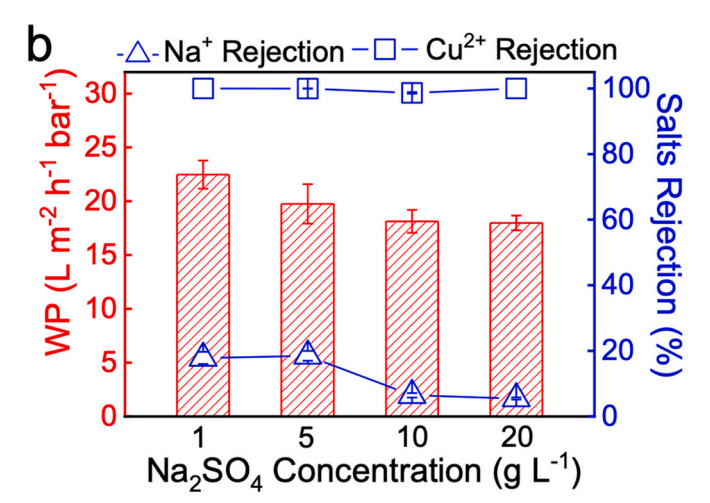
of heavy metal ions [7]. Thus, a given ion with a higher diffusivity is more likely to diffuse through the membrane. The diffusion coefficient of the remaining three ions is displayed in Table 2, showing the order  $Pb^{2+} > Zn^{2+} > Ni^{2+}$ . However, the three cross-linked P84/PEI membranes have a higher rejection of Pb<sup>2+</sup>, the ion with the highest diffusion coefficient. Therefore, the diffusion of cations is not considered the dominant role in determining the separation efficiency in a positively charged membrane. It should be noted that the anions of the heavy metal salts used in this work are chloride and nitrate. Compared with divalent heavy metal cations, H<sup>+</sup> has a smaller charge and a smaller size, making it is easier to pass through the membrane to achieve the charge balance with Cl<sup>-</sup> or NO<sub>3</sub><sup>-</sup> in the permeate solutions [7]. Therefore, more hydroxide ions and metal cations would be retained and accumulated near the membrane surface. As a result, Cu(OH)<sub>2</sub>, Pb(OH)<sub>2</sub>, Zn(OH)<sub>2</sub>, and Ni(OH)<sub>2</sub> precipitates would be generated when the solubility of these metal hydroxides is reached. Table S2 summarizes the solubility product constant, K<sub>sp</sub>, of these metal hydroxides. K<sub>sp</sub> is an equilibrium constant that describes the extent to which an ionic compound dissolves in water. The lower the K<sub>sp</sub> value of a solute, the less soluble it is in a solution. K<sub>sp</sub> values of the metal hydroxides are in a sequence of Ni  $(OH)_2 > Pb(OH)_2 > Zn(OH)_2 > Cu(OH)_2$ . The  $K_{sp}$  of  $Cu(OH)_2$  is four orders of magnitude lower than others, explaining the high rejection of Cu<sup>2+</sup>. This is mainly because Cu<sup>2+</sup> tends to precipitate and generate a cake layer of Cu(OH)<sub>2</sub> precipitate near the membrane surface. This observation was also described by Hilal et al. [36]. Indeed, blue color can be observed on the membrane surface after filtration. Vice versa, Ni  $(OH)_2$  has the highest  $K_{sp}$  of the others, indicating a higher solubility of nickel in water. Thus, Ni<sup>2+</sup> tends to diffuse the membrane giving rise to a lower rejection of  $Ni^{2+}$ . However, the difference of the  $K_{sp}$  between Zn $(OH)_2$  and  $Pb(OH)_2$  is negligible. Instead, the hydration radius of  $Pb^{2+}$  is much smaller than that of Zn2+. A lower hydration radius of ion probably has a stronger electrostatic repulsion between the positively charged membrane surface and the charged ions, resulting in a higher rejection. This may explain the higher retention of  $Pb^{2+}$  than  $Zn^{2+}$ . These results imply that the separation of heavy metal ions of the positively charged P84/PEI membrane is a synergistic effect of precipitation and electrostatic repulsion.

#### 3.4. Membrane separation performance with different salt concentrations

Selective removal of trace heavy metal elements from saline water is typically challenging for nanofiltration membranes. To this end, the newly developed positively charged P84/PEI nanofiltration membrane was evaluated in multi-component saline water. Cu<sup>2+</sup> was chosen as the representative heavy metal ion with a concentration of 10 ppm. Na<sub>2</sub>SO<sub>4</sub>  $(1, 5, 10, \text{ and } 20 \text{ g L}^{-1})$  was used as the salt solute. Fig. 9 presents the selective removal performance of three P84/PEI membranes for Cu<sup>2+</sup> from the brine water. As the Na<sub>2</sub>SO<sub>4</sub> concentrations increased, the flux of the three P84/PEI membranes decreased simultaneously. This might be attributed to the increased osmotic pressure in the feed side [37]. The three P84/PEI membranes have a low rejection of Na<sub>2</sub>SO<sub>4</sub> due to the Donnan exclusion. As the Na<sub>2</sub>SO<sub>4</sub> concentration increased, there was an increasing shielding effect caused by the reduced membrane surface potential, and therefore, the rejection of Na<sub>2</sub>SO<sub>4</sub> further decreased [38]. In addition, the rejection of Cu<sup>2+</sup> by all membranes is greater than 98%. Taking Na<sub>2</sub>SO<sub>4</sub> concentration of 10 g L<sup>-1</sup> as an example, it was found that the 20%P84/PEI membrane has the best performance for separating  $Cu^{2+}$  from saline water (i.e., water permeance: 23.0  $\pm$  0.9 L m<sup>-2</sup> h<sup>-1</sup> bar<sup>-1</sup>; Na<sub>2</sub>SO<sub>4</sub> rejection: 5.2  $\pm$  0.9%; Cu<sup>2+</sup> rejection: 98.2  $\pm$  0.2%). In contrast, the 24%P84/PEI membrane has an excellent selectivity but a low water permeance (the highest Cu<sup>2+</sup> rejection >99%, Na<sub>2</sub>SO<sub>4</sub> rejection of 22.9  $\pm$  1.9%, and water permeance of 8.4  $\pm$  1.0 L m $^{-2}$  h $^{-1}$ bar<sup>-1</sup>), suggesting that the 20%P84/PEI membrane could efficiently remove Cu<sup>2+</sup> while allowing the passage of Na<sub>2</sub>SO<sub>4</sub>. It is fascinating that the positively charged P84/PEI nanofiltration membrane can be potentially used for the selective removal of Cu<sup>2+</sup> cations from highly saline water with salt concentration up to 20 g  $L^{-1}$ .

Furthermore, the feed solution was extended to four different heavy metal ions, namely Cu<sup>2+</sup>, Zn<sup>2+</sup>, Ni<sup>2+</sup>, and Pb<sup>2+</sup>. The saline water containing 10 g L<sup>-1</sup> of Na<sub>2</sub>SO<sub>4</sub> and 10 ppm of each heavy metal ion was used as the feed solution. As shown in Fig. 10, the 20%P84/PEI and the 22% P84/PEI membrane have a similar Cu<sup>2+</sup> rejection but very low rejections of Zn<sup>2+</sup>, Ni<sup>2+</sup>, and Pb<sup>2+</sup>. One possible explanation is that the adsorbed dual charged (SO<sub>4</sub><sup>2-</sup>) ions shield the surface charge of the membrane, leading to a high salt permeation [38,39]. In this case, size exclusion is the key factor in the hindrance of heavy metal ions. The mean pore radius of 20%P84/PEI (0.474 nm) and 22%P84/PEI (0.426 nm) membranes is larger than the hydrated radii of  $\mbox{Pb}^{2+}$  (0.401 nm),  $\mbox{Ni}^{2+}$  (0.404 nm),  $\mathrm{Zn}^{2+}$  (0.430 nm) and  $\mathrm{Cu}^{2+}$  (0.419 nm), causing diffusion of ions through the membrane. The 24%P84/PEI membrane has a small mean pore radius of 0.389 nm, smaller than the heavy metal ions. Interestingly, all three membranes have a high Cu<sup>2+</sup> rejection. On the one hand, as mentioned above, Cu(OH)2 precipitates would be produced when the solubility of these metal hydroxides is reached. On the other hand, metal ion/PEI complexes would form near the membrane surface [41]. The stability constant of the PEI/Cu complex is higher than that of other complexes [41,42]. These factors together contribute to a specific selection of Cu<sup>2+</sup> by the membrane. The filtration was measured in a noncyclic operation mode, resulting in an increasing ionic strength in the feed solution [43]. Similar studies have also shown that PEI-based membranes have a high selectivity to copper ions due to the combination of electrostatic repulsion and adsorption [44]. In summary, the 20% P84/PEI and 22%P84/PEI membranes can be used in (1) removal of simple components of heavy metal from wastewater and (2) selective removal of Cu<sup>2+</sup> containing wastewater. The 24%P84/PEI membrane is the best membrane for dealing with complex heavy metals in saline water.





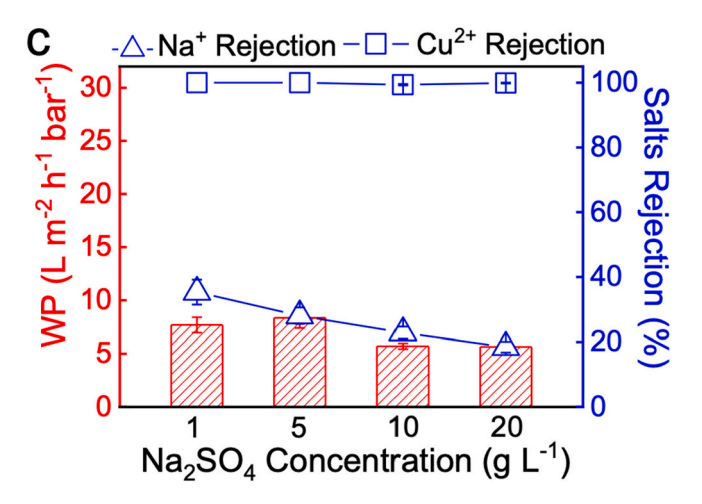
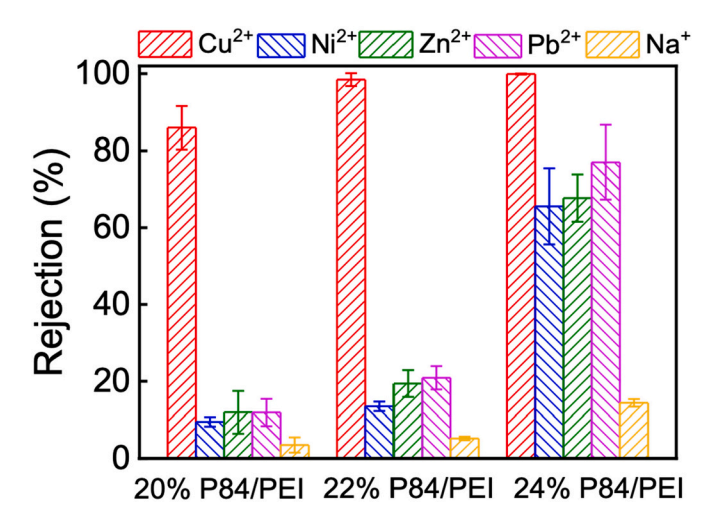


Fig. 9. Separation performance with 10 ppm  ${\rm Cu}^{2+}$  in various  ${\rm Na_2SO_4}$  concentrations at 25 °C and 8 bar. (a) 20%P84/PEI membrane; (b) 22%P84/PEI membrane; (c) 24%P84/PEI membrane.

#### 4. Conclusion

Overall, three positively charged nanofiltration membranes were developed by PEI cross-linking on the top layer of a P84 substrate. The membrane pore size was tailored by changing the content of P84 polymer in the casting solutions. The rejection of inorganic salts follows a sequence  $MgCl_2>MgSO_4>NaCl>Na_2SO_4$ . Besides, all the PEI cross-



**Fig. 10.** Separation performance with four heavy metal ions ( $Cu^{2+}$ ,  $Zn^{2+}$ ,  $Ni^{2+}$  and  $Pb^{2+}$ , 10 ppm for each type) in 10 g  $L^{-1}$  of the  $Na_2SO_4$  solution at 25 °C and 8 bar.

linked membranes have a high rejection of four types of heavy metal salts (ZnCl<sub>2</sub>, PbCl<sub>2</sub>, Ni(NO<sub>3</sub>)<sub>2</sub>, and Cu(NO<sub>3</sub>)<sub>2</sub>) in a single-salt filtration due to the highly positively charged membrane surface. The 20%P84/PEI and 22%P84/PEI membranes show high pure water permeance of 27.7  $\pm$  1.5 and 23.0  $\pm$  1.2 L m $^{-2}$  h $^{-1}$  bar $^{-1}$ , respectively. These two membranes can be selectively removing and concentrating copper ions from highly salty solutions (1–20 g L $^{-1}$ ). Moreover, the 24%P84/PEI membrane with a small mean pore radius shows great potential for separating heavy metals from saline water.

# CRediT authorship contribution statement

Bart Van der Bruggen and Yi Li designed the research. Junfeng Zheng and Xin Zhang performed the experiments. Guichuan Li and Guanghai Fei performed SEM measurement. Pengrui Jin and Yanling Liu helped to revise the paper. Christine Wouters performed ICP-MS measurement. Glen Meir performed HPLC measurement. Junfeng Zheng, Xin Zhang, Pengrui Jin, Yanling Liu, Yi Li, and Bart Van der Bruggen co-wrote the paper.

# Declaration of competing interest

The authors declare that they have no known competing financial interests or personal relationships that could have appeared to influence the work reported in this paper.

### Acknowledgements

Junfeng Zheng acknowledges the financial support from the China Scholarship Council of the Ministry of Education of China.

# Appendix A. Supplementary data

Supplementary data to this article can be found online at https://doi.org/10.1016/j.desal.2021.115380.

### References

- R.L. Chaney, The heavy elements: chemistry, environmental impact, and health effects, J. Environ. Qual. 20 (1991) 876.
- [2] B. Southichak, K. Nakano, M. Nomura, N. Chiba, O. Nishimura, Phragmites australis: a novel biosorbent for the removal of heavy metals from aqueous solution, Water Res. 40 (2006) 2295–2302.

- [3] Y.C. Jordan, A. Ghulam, S. Hartling, Traits of surface water pollution under climate and land use changes: a remote sensing and hydrological modeling approach, EarthSci. Rev. 128 (2014) 181-195.
- [4] Q.S. Li, S.S. Cai, C.H. Mo, B. Chu, L.H. Peng, F.B. Yang, Toxic effects of heavy metals and their accumulation in vegetables grown in a saline soil, Ecotoxicol. Environ. Saf. 73 (2010) 84-88.
- [5] C. Sgarlata, G. Arena, E. Longo, D. Zhang, Y. Yang, R.A. Bartsch, Heavy metal separation with polymer inclusion membranes, J. Membr. Sci. 323 (2008)
- [6] N. Abdullah, N. Yusof, W.J. Lau, J. Jaafar, A.F. Ismail, Recent trends of heavy metal removal from water/wastewater by membrane technologies, J. Ind. Eng. Chem. 76
- [7] J. Tian, H. Chang, S. Gao, R. Zhang, How to fabricate a negatively charged NF membrane for heavy metal removal via the interfacial polymerization between PIP and TMC? Desalination 491 (2020), 114499.
- [8] J. Zheng, M. Li, Y. Yao, X. Zhang, L. Wang, Zwitterionic carbon nanotube assisted thin-film nanocomposite membranes with excellent efficiency for separation of mono/divalent ions from brackish water, J. Mater. Chem. A 5 (2017) 13730-13739.
- [9] J. Zheng, M. Li, K. Yu, J. Hu, X. Zhang, L. Wang, Sulfonated multiwall carbon nanotubes assisted thin-film nanocomposite membrane with enhanced water flux and anti-fouling property, J. Membr. Sci. 524 (2017) 344-353.
- [10] J. Zheng, Y. Liu, J. Zhu, P. Jin, T. Croes, A. Volodine, S. Yuan, B. Van der Bruggen, Sugar-based membranes for nanofiltration, J. Membr. Sci. 619 (2021), 118786.
- [11] J. Schaep, B. Van der Bruggen, C. Vandecasteele, D. Wilms, Influence of ion size and charge in nanofiltration, Sep. Purif. Technol. 14 (1998) 155–162.

  [12] K.H. Choo, D.J. Kwon, K.W. Lee, S.J. Choi, Selective removal of cobalt species
- using nanofiltration membranes, Environ. Sci. Technol. 36 (2002) 1330-1336.
- [13] Y. Zhang, S. Zhang, T.S. Chung, Nanometric graphene oxide frame work membranes with enhanced heavy metal removal via nanofiltration, Environ. Sci. Technol. 49 (2015) 10235-10242.
- [14] S. Lee, E. Lee, J. Ra, B. Lee, S. Kim, S.H. Choi, S.D. Kim, J. Cho, Characterization of marine organic matters and heavy metals with respect to desalination with RO and NF membranes, Desalination 221 (2008) 244–252.
- [15] K. Gu, S. Wang, Y. Li, X. Zhao, Y. Zhou, C. Gao, A facile preparation of positively charged composite nanofiltration membrane with high selectivity and permeability, J. Membr. Sci. 581 (2019) 214–223.
- [16] Y.C. Chiang, Y.Z. Hsub, R.C. Ruaan, C.J. Chuang, K.L. Tung, Nanofiltration membranes synthesized from hyperbranched polyethyleneimine, J. Membr. Sci. 326 (2009) 19–26.
- [17] H.Z. Zhang, Z.L. Xu, H. Ding, Y.J. Tang, Positively charged capillary nanofiltration membrane with high rejection for Mg<sup>2+</sup> and Ca<sup>2+</sup> and good separation for Mg<sup>2+</sup> and Li<sup>+</sup>, Desalination 420 (2017) 158–166.
- [18] J. Gao, S.P. Sun, W.P. Zhu, T.S. Chung, Green modification of outer selective P84 nanofiltration (NF) hollow fiber membranes for cadmium removal, J. Membr. Sci. 499 (2016) 361-369.
- [19] J. Song, T. Huang, H. Oiu, X. Niu, X.M. Li, Y. Xie, T. He, A critical review on membrane extraction with improved stability: potential application for recycling metals from city mine, Desalination 440 (2018) 18-38.
- [20] J. Zhu, S. Yuan, A. Uliana, J. Hou, J. Li, X. Li, M. Tian, Y. Chen, A. Volodin, B. Van der Bruggen, High-flux thin film composite membranes for nanofiltration mediated by a rapid co-deposition of polydopamine/piperazine, J. Membr. Sci. 554 (2018) 97-108
- [21] J. Ding, H. Wu, P. Wu, Development of nanofiltration membranes using musselinspired sulfonated dopamine for interfacial polymerization, J. Membr. Sci. 598 (2020) 117658.
- [22] C.Y. Zhu, C. Liu, J. Yang, B.B. Guo, H.N. Li, Z.K. Xu, Polyamide nanofilms with linearly-tunable thickness for high performance nanofiltration, J. Membr. Sci. 627 (2021), 119142.
- [23] G. Hurwitz, G.R. Guillen, E.M.V. Hoek, Probing polyamide membrane surface charge, zeta potential, wettability, and hydrophilicity with contact angle measurements, J. Membr. Sci. 349 (2010) 349-357.

- [24] W. Zhang, X. Zhang, Effective inhibition of gypsum using an ion-ion selective nanofiltration membrane pretreatment process for seawater desalination, J. Membr. Sci. 632 (2021), 119358.
- [25] Y. Li, E. Wong, A. Volodine, C. Van Haesendonck, K. Zhang, B. Van Der Bruggen, Nanofibrous hydrogel composite membranes with ultrafast transport performance for molecular separation in organic solvents, J. Mater. Chem. A 7 (2019) 19269-19279.
- [26] C. Ba, J. Langer, J. Economy, Chemical modification of P84 copolyimide membranes by polyethylenimine for nanofiltration, J. Membr. Sci. 327 (2009)
- J. Gao, S.P. Sun, W.P. Zhu, T.S. Chung, Polyethyleneimine (PEI) cross-linked P84 nanofiltration (NF) hollow fiber membranes for Pb2+ removal, J. Membr. Sci. 452 (2014) 300-310
- [28] X. You, H. Wu, R. Zhang, Y. Su, L. Cao, Q. Yu, J. Yuan, K. Xiao, M. He, Z. Jiang, Metal-coordinated sub-10 nm membranes for water purification, Nat. Commun. 10 (2019) 1-10.
- [29] Y. Yao, C. Ba, S. Zhao, W. Zheng, J. Economy, Development of a positively charged nanofiltration membrane for use in organic solvents, J. Membr. Sci. 520 (2016)
- [30] Z. Zhang, G. Kang, H. Yu, Y. Jin, Y. Cao, Fabrication of a highly permeable composite nanofiltration membrane via interfacial polymerization by adding a novel acyl chloride monomer with an anhydride group, J. Memb. Sci. 570-571 (2019) 403-409.
- [31] M. Sun, M. Li, P. Wang, X. Zhang, C. Wu, Y. Wu, Production of N-2hydroxyethylpiperazine-N"-2-ethanesulfonic acid by BMED process using porous P84 co-polyimide membranes, Chem. Eng. Res. Des. 137 (2018) 467–477
- [32] P. Xu, W. Wang, X. Qian, H. Wang, C. Guo, N. Li, Z. Xu, K. Teng, Z. Wang, Positive charged PEI-TMC composite nanofiltration membrane for separation of Li+ and Mg2+ from brine with high Mg2+/Li+ ratio, Desalination 449 (2019) 57–68.
- [33] G. Zhao, R. Hu, X. Zhao, Y. He, H. Zhu, High flux nanofiltration membranes prepared with a graphene oxide homo-structure, J. Membr. Sci. 585 (2019) 29–37.
- [34] W.P. Zhu, J. Gao, S.P. Sun, S. Zhang, T.S. Chung, Poly(amidoamine) dendrimer (PAMAM) grafted on thin film composite (TFC) nanofiltration (NF) hollow fiber membranes for heavy metal removal, J. Membr. Sci. 487 (2015) 117-126.
- M. Li, Y. Yao, W. Zhang, J. Zheng, X. Zhang, L. Wang, Fractionation and concentration of high-salinitytextilewastewater using an ultrapermeablesulfonatedthin-filmcomposite, Environ. Sci. Technol. 51 (2017) 9252-9260.
- [36] B.A.M. Al-Rashdi, D.J. Johnson, N. Hilal, Removal of heavy metal ions by nanofiltration, Desalination 315 (2013) 2-17.
- [37] B. Van Der Bruggen, B. Daems, D. Wilms, C. Vandecasteele, Mechanisms of retention and flux decline for the nanofiltration of dye baths from the textile industry, Sep. Purif. Technol. 22 (2001) 519-528.
- [38] Y. Liu, Y. Zhao, X. Wang, X. Wen, X. Huang, Y.F. Xie, Effect of varying piperazine concentration and post-modification on prepared nanofiltration membranes in selectively rejecting organic micropollutants and salts, J. Membr. Sci. 582 (2019) 274-283.
- [39] Y. Xu, J. Lin, C. Gao, B. Van Der Bruggen, Q. Shen, H. Shao, J. Shen, Preparation of high-flux nanoporous solvent resistant polyacrylonitrile membrane with potential fractionation of dyes and  $\rm Na_2SO_4$ , Ind. Eng. Chem. Res. 56 (2017) 11967–11976.
- [41] F. Smail, O. Arous, M. Amara, H. Kerdjoudj, A competitive transport across polymeric membranesStudy of complexation and separation of ions, Comptes Rendus Chimie 16 (2013) 605-612.
- [42] M. Ulewicz, E. Radzyminska-Lenarcik, Supported liquid (SLM) and polymerinclusion (PIM) membrane spertraction of Copper(II) from aqueous nitrate solutions by 1-Hexyl-2-methylimidazole, Sep. Sci. Technol. 47 (2012) 1383–1389.
- $\hbox{\bf [43]}\ \ M.I.\ Baoxia,\ M.\ Elimelech,\ Gypsum\ scaling\ and\ cleaning\ in\ forward\ osmosis:$ measurements and mechanisms, Environ. Sci. Technol. 44 (2010) 2022-2028.
- J. Wang, W. Yu, N.J.D. Graham, L. Jiang, Evaluation of a novel polyamidepolyethylenimine nanofiltration membrane for wastewater treatment: removal of <sup>+</sup> ions, Chem. Eng. J. 392 (2020).
- [45] J. Zheng, L. Yi, X. Daliang, Z. Rui, L. Yanyan, et al., Facile fabrication of a positively charged nanofiltration membrane for heavy metal and dye removal, Sep. Sci. Technol. 282 (2022) 120155.